



N^2 -Trimethylacetyl substituted and unsubstituted- N^4 -phenylsubstituted-6-(2-pyridin-2-ylethyl)-7H-pyrrolo[2,3-d]pyrimidine-2,4-diamines: Design, cellular receptor tyrosine kinase inhibitory activities and in vivo evaluation as antiangiogenic, antimetastatic and antitumor agents



Aleem Gangjee^{a,*}, Ojas A. Namjoshi^a, Jianming Yu^a, Michael A. Ihnat^b,
Jessica E. Thorpe^b, Lora C. Bailey-Downs^b

^a Division of Medicinal Chemistry, Graduate School of Pharmaceutical Sciences, Duquesne University, Pittsburgh, PA 15282, United States

^b Department of Pharmaceutical Sciences, The University of Oklahoma College of Pharmacy, Oklahoma City, OK 73117, United States

ARTICLE INFO

Article history:

Received 21 August 2012

Revised 6 December 2012

Accepted 14 December 2012

Available online 10 January 2013

Keywords:

Antiangiogenic

Antimetastatic

In vivo

Sonogashira coupling

ABSTRACT

Six novel N^4 -phenylsubstituted-6-(2-pyridin-2-ylethyl)-7H-pyrrolo[2,3-d]pyrimidine-2,4-diamines and their N^2 -trimethylacetyl substituted analogs were synthesized as receptor tyrosine kinase (RTK) inhibitors. A microwave-mediated Sonogashira reaction was used as a key step for the synthesis of these compounds. Biological evaluation, in whole cell assays, showed that some analogs had remarkable inhibitory activity against a variety of RTKs and in particular cytotoxic activity against A431 tumor cells in culture. The inhibitory data against RTKs in this study demonstrated that variation of the 4-anilino substituents of these analogs dictates both potency and specificity of inhibitory activity against various RTKs. The study also supported the hypothesis that interaction of substituents on the 2-amino group with hydrophobic site-II provides an increase in potency. Compound **8** of this series was selected for evaluation in vivo in a B16-F10 syngeneic mouse tumor model and exhibited significant reduction in tumor growth rate, in tumor vascular density and in metastases to the lung compared to the control.

© 2013 Elsevier Ltd. All rights reserved.

1. Introduction

Receptor tyrosine kinases (RTKs) are a subfamily of protein tyrosine kinases, which play key roles in tumor growth, survival and dissemination. A variety of growth factors particularly vascular endothelial growth factor (VEGF), epithelial growth factor (EGF), platelet derived growth factor (PDGF), and their receptors are over-expressed in several tumors. These growth factors and their receptors are directly as well as indirectly involved in cancer.¹

Angiogenesis, the formation of new blood vessels from existing vasculature, in solid tumors is essential for both physiologic and pathologic processes. It is a complex cascade that is tightly regulated by proangiogenic and antiangiogenic factors.² VEGF is the

Abbreviations: RTK, receptor tyrosine kinase; EGFR, epithelial growth factor receptor; VEGFR, vascular endothelial growth factor receptor; PDGFR, platelet derived growth factor receptor; CAM, chorioallantoic membrane; Abl, abelson tyrosine kinase; CML, chronic myelogenous leukemia; GIST, gastrointestinal stromal tumors; FLT3, FMS-like tyrosine kinase 3; MTX, methotrexate; ELISA, enzyme-linked immunosorbent assay.

* Corresponding author. Tel.: +1 412 396 6070; fax: +1 412 396 5593.

E-mail address: gangjee@duq.edu (A. Gangjee).

predominant mediator of angiogenesis.^{3,4} The expression of VEGF is efficiently controlled under physiologic conditions. However, VEGF is secreted by a large number of tumor cells, leading to angiogenesis that promotes tumor growth and metastases. In addition to VEGF, several external factors are also involved in stimulating tumor angiogenesis. Some of the principal proangiogenic regulators include growth factors EGF, PDGF, fibroblast growth factor (FGF), insulin-like growth factor-1 (IGF-1), transforming growth factors ($TGF\alpha$ and β) and tumor necrosis factor α (TNF- α) among others.⁵ The newly sprouted blood vessels provide an additional supply of nutrients to the tumor to grow beyond 1–2 mm.³ Angiogenesis is a pivotal step in the transition of some solid tumors from a dormant state to a malignant state; it also provides metastatic pathways for solid tumors.⁶ In addition, angiogenesis contributes to the development of hematologic malignancies, particularly multiple myeloma, leukemia, and lymphoma. However, the role of angiogenesis has not been clearly defined in hematologic malignancies.^{7–9} Angiogenesis has been described as one of the hallmarks of cancer.¹⁰ Thus inhibition of tumor angiogenesis affords attractive targets for the development of antitumor agents.

There has been considerable discussion in the literature regarding the use of RTK inhibitors as monotherapy for cancer or the combination of multiple RTK inhibitors either as single agents or in combination with other chemotherapeutic agents. The majority of earlier reports underlined the development of small molecule targeted therapy against single RTK (Fig. 1), some of which afforded clinical agents such as gefitinib (**1**)¹¹ and erlotinib (**2**).¹¹ However, tumors have redundant signaling pathways for angiogenesis and often develop resistance to agents that target single specific pathways.¹² Recently, crosstalk has been implicated between EGFR and other growth factor receptors involved in tumorigenesis.⁵ Hence to arrest angiogenesis, a multifaceted approach that targets multiple signaling pathways has been shown to be more effective than the inhibition of a single target. The most important consequence of inhibiting multiple RTKs is to retard tumor resistance by also blocking potential 'escape routes'. Since RTKs are present in endothelial cells (VEGFR, PDGFR), tumor cells (FGFR, PDGFR), and pericytes/smooth muscle cells (FGFR, PDGFR), inhibition of more than one RTKs provides synergistic inhibitory effects against solid tumors.¹² Recently, VEGFR-2 and PDGFR- β have been implicated in controlling angiogenesis at two different stages of the angiogenic process, and it has been shown that inhibition of VEGFR-2 and PDGFR- β with two separate inhibitors produces a synergistic effect in early stage as well as late stage pancreatic islet cancer in mouse models by attacking the angiogenic process at two different sites.^{13,14}

A flood of reports on the design of multikinase inhibitors have appeared in the past few years,^{1,5,13–16} some of which have led to clinically approved agents (Fig. 1) such as imatinib (**3**),¹⁷ sunitinib (**4**),¹⁸ sorafenib (**5**),¹⁹ and lapatinib (**6**) (Fig. 1).²⁰

2. Results and discussion

2.1. Design of inhibitors

The aim of this study was to design multikinase inhibitors, thus a general RTK pharmacophore model was utilized rather than the X-ray crystal structures of specific RTKs.^{21,22} As shown in this general pharmacophore model depicted in Figure 2, the 2-amino group is strategically incorporated in our pyrrolo[2,3-*d*]pyrimidine scaffold to afford an additional hydrogen-bond contact with the backbones of the hinge region amino acids.²³ This places the 2-amino

pyrrolo[2,3-*d*]pyrimidine scaffold in the ATP binding pocket of RTKs in at least three different binding modes (Fig. 2). In these different modes, the side chain substituents are oriented in different sites in the ATP binding domain, the hydrophobic site I, sugar binding pocket or the phosphate binding region (Fig. 2).

The presence of a 2-pyridyl side chain makes these compounds of further interest. These analogs are slightly more polar ($clogP \approx 3.5$) than the corresponding phenyl substituted analogs ($clogP \approx 4.5$) reported earlier.²² This may help in cellular transport of the molecules by altering the lipid/water solubility ratio. The compounds are also amenable to acid salt formation (pyridyl ring $pK_a \approx 5.2$ – 5.4) and provide increased water solubility as acid salts for ease of administration.

Various aniline substituents at the 4-position that were reported in the literature to provide potent RTK inhibitors^{11,24–30} were incorporated in the design of **7–12** to determine their effects on potency and/or selectivity against RTKs. Compound **7** was designed with a 3-Br substituted aniline at the 4-position as similar substituents have shown^{26,27} good EGFR inhibition in quinazolines. Compound **8** was designed with a 3-Br, 4-F substituted aniline at the 4-position as a logical step from **7** and as a prior analog to compound **9** with a 3-Cl, 4-F substituted aniline moiety. This aniline has been shown to improve EGFR inhibition by Wissner et al.²⁸ in the case of quinazolines. Most importantly, gefitinib (**1**, Fig. 1) also has a 3-Cl, 4-F substituted aniline. In a recent crystal structure report²⁹ of gefitinib (**1**) with EGFR it was found that the 3-Cl group fits snugly in a pocket formed by the side chains of residues Lys745, Leu788 and Thr790. The 4-F substituent extends toward the side chains of Leu788, Met766 and Glu762. Thus 3-Cl, 4-F substituted aniline was included in our design to determine its effect on EGFR inhibition and to possibly extend the spectrum of RTK inhibition of these compounds. The 3-ethynylaniline substituent of **10** was similar to that of erlotinib (**2**, Fig. 1). As reported in the crystal structure of erlotinib (**2**) bound with EGFR, the acetylene moiety is within 4 Å distance from side chains of Thr766, Lys721, and Leu764 thus possibly forming hydrophobic interactions leading to improved binding of erlotinib with EGFR. The 3-trifluoromethyl group of **11** was included because electronegative groups at the *meta*-position of the aniline moiety are better for EGFR inhibitory activity as previously noted in the structure–activity relationship studies of quinazoline compounds by Rewcastle et al.²⁶ and Bridges et al.²⁷ Additionally Manley et al.³⁰ has shown,

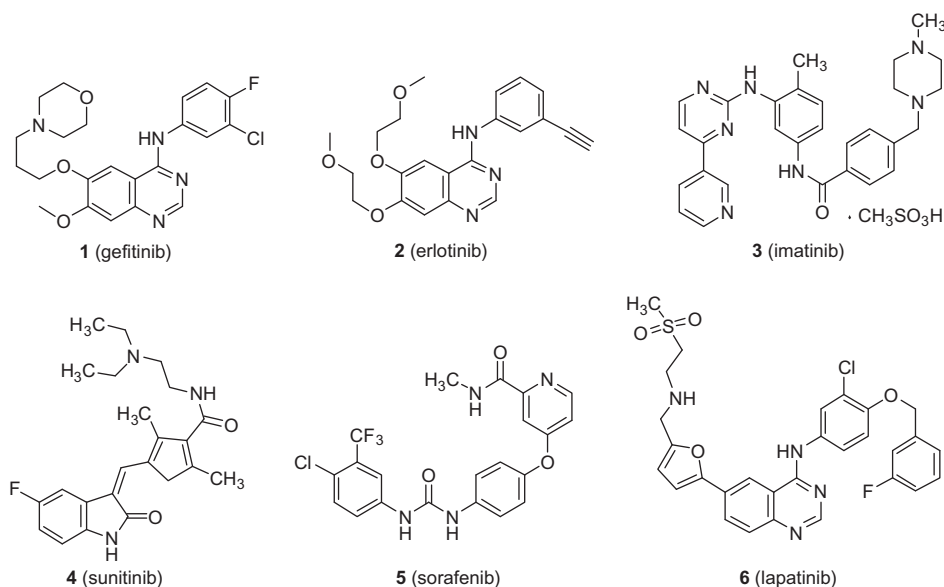


Figure 1. Structures of RTK inhibitors in market.

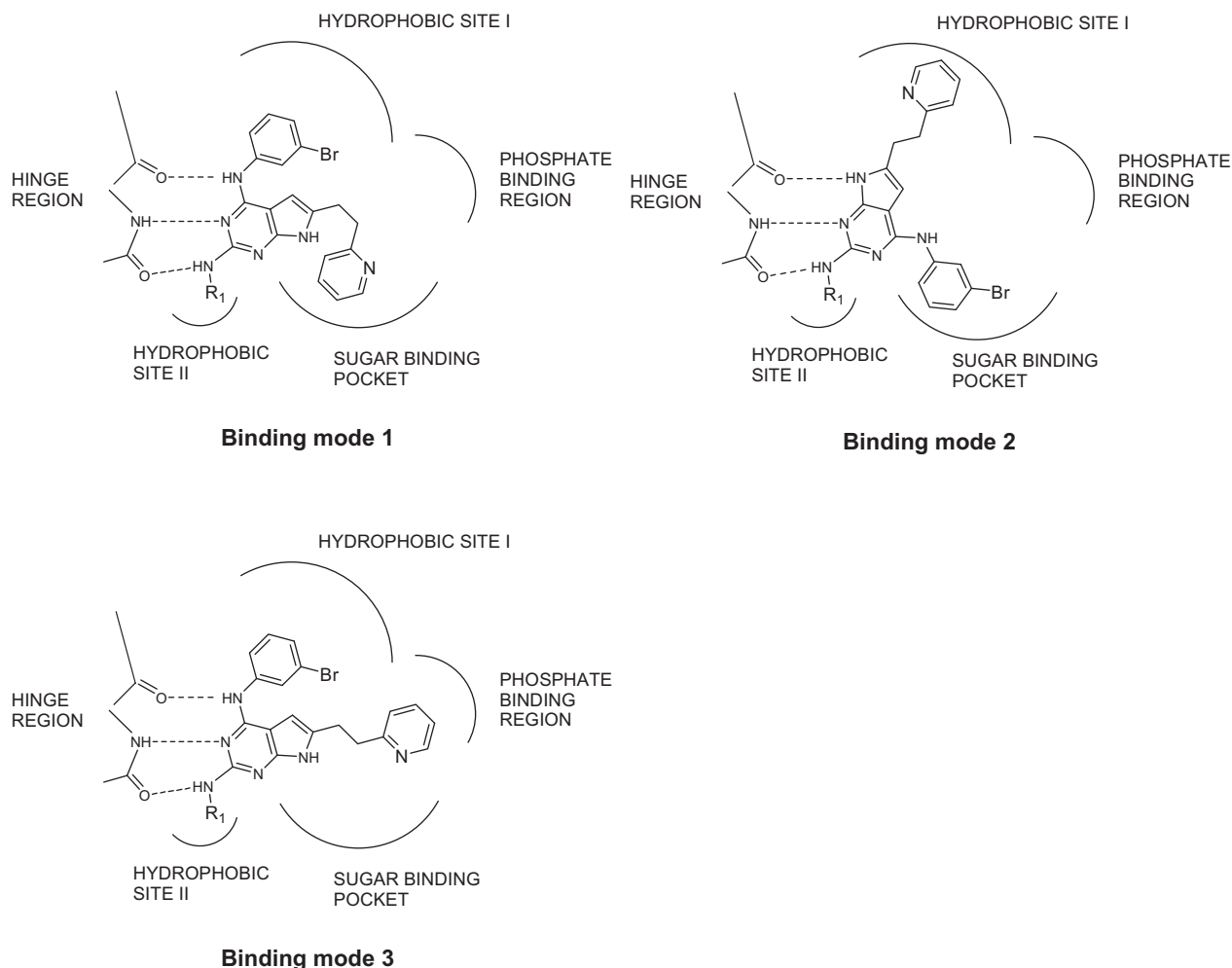


Figure 2. General pharmacophore model of pyrrolo[2,3-d]pyrimidines.

in the anthranilic acid amide series of compounds, that the 3-trifluoromethyl substituted compound shows excellent inhibition of VEGFR and was a potent antiangiogenic agent. Thus **11** was designed with the idea that it may inhibit both EGFR as well as VEGFR thus affording dual RTK inhibition. Compound **12** is an analog of **11** with a small electronegative fluoro substituent at the 4-position of the aniline to further improve EGFR inhibitory activity.²⁷

In addition to the 2-NH₂ moiety providing additional H-bonding with the hinge region,²³ substituents on the 2-amino group could afford access to the hydrophobic site II and perhaps improve the potency against RTKs. As shown in Figure 2, compound **7** makes three H-bond contacts with the hinge region of the ATP binding pocket. In this binding mode, substituents on the 2-amino group could access the hydrophobic site 2 and perhaps improve the potency against RTKs. In EGFR the hydrophobic site 2 is formed by Leu694 and Gly772. Thus, in this study, a trimethylacetyl group on the 2-amino moiety was incorporated as an initial attempt to explore this hypothesis in compounds **14–18** (Fig. 3). The substituents on the 4-anilino ring for **14–18** were kept the same as in **8–12**, respectively for direct comparison.

2.2. Chemistry

The syntheses of compounds **13–18** and **7–12** are shown in Scheme 1. Intermediate **21** can be obtained by a Sonogashira coupling of **19** with 2-ethynylpyridine **20**.³¹ However the reported conditions for this conversion required the reaction to be stirred

at room temperature for 72 h and afforded poor yields (49%).³¹ Thus it was necessary to optimize the reaction conditions for the synthesis of **21**.

As shown in Table 1 the reaction was very sluggish at room temperature (entry 1). The reaction did not proceed in less polar solvent - THF (entry 2), probably due to inferior solubility. In acetonitrile the reaction did not go to completion even after stirring for 72 h at room temperature (entry 3). Prolonged heating at 100 °C in DMF led to inferior results (entry 4). Hence a microwave mediated reaction approach was utilized. Under microwave irradiation maintaining the temperature at 100 °C for 1 h a spot corresponding to the product was observed on TLC (entry 5). However the reaction did not reach completion and unreacted starting material was observed on TLC. At higher temperature (180 °C) some decomposition products (baseline spot on TLC) were observed on TLC. Slightly better results were obtained when the catalyst was generated in situ instead of the preformed catalyst and the reaction was run at 100 °C for 1 h (entry 7). Higher temperature (150 °C) improved the conversion, but also led to some decomposition products (baseline spot on TLC). Decreasing the reaction time to 10 min improved the yield considerably (entry 9). Tweaking the reaction time further led to the optimized condition in which the reaction proceeded smoothly under microwave irradiation at 150 °C in 3.5 min (entry 10). Additionally, the use of in situ generated catalyst proved to be more efficient instead of a pre-formed catalyst such as tetrakis(triphenyl)phosphinepalladium (0) (compare entry 11 with entry 10) (Table 1).

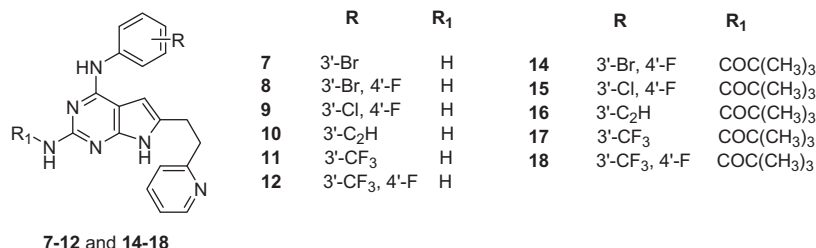
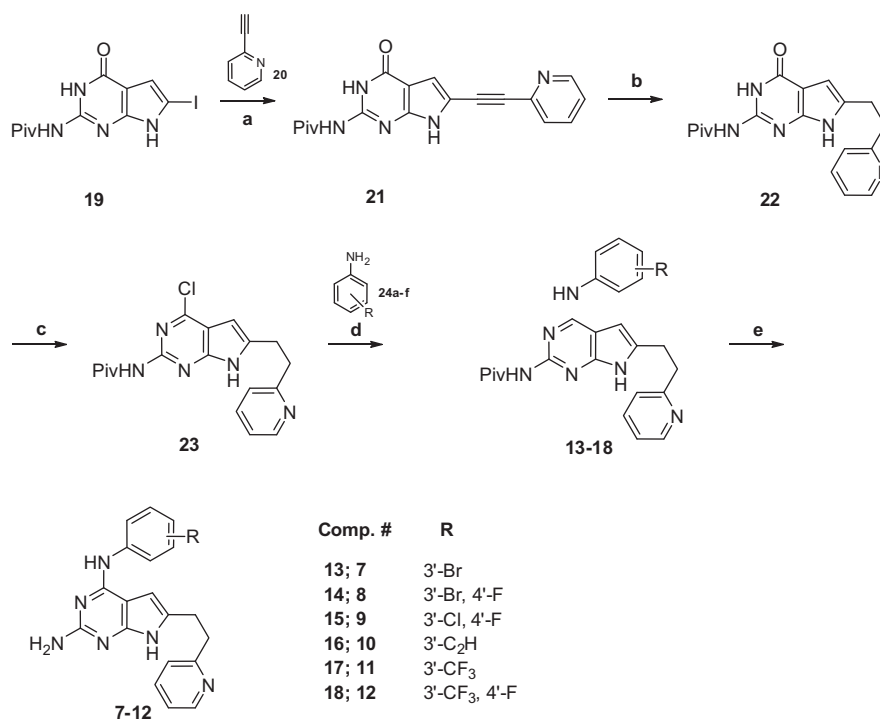


Figure 3. Designed compounds.



Scheme 1. Synthesis of target compounds.

Compound **21** was obtained from **19** via a microwave-mediated Sonogashira reaction. Catalytic reduction of the triple bond of **21** with 5% Palladium on charcoal afforded **22** in 75% yield. Chlorination of **22** with phosphorus oxychloride afforded **23** in 70% yield. Compound **23** was reacted with appropriately substituted anilines **24a–f** in isopropanol at reflux in the presence of 2 drops of concd HCl for 3 h to afford **13–18** in 80–95% yields. Deprotection of the 2-amino groups of **13–18** with 1 N NaOH in methanol followed by chromatographic purification afforded **7–12**.

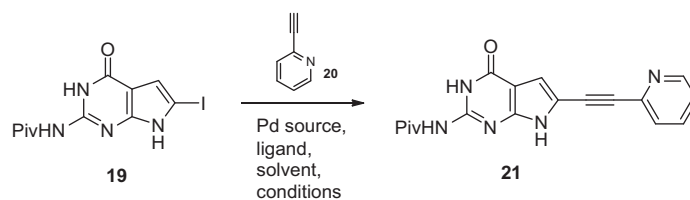
2.3. In vitro evaluation for kinase inhibition, A431 cytotoxicity and CAM angiogenesis inhibition

RTK inhibitory activity of compounds **7–12** and intermediates **14–18** were evaluated using human tumor cells known to express high levels of EGFR, VEGFR-1, VEGFR-2, and PDGFR- β using a phosphotyrosine ELISA cytotblot (Table 2).^{32,33} Compounds known to inhibit a particular RTK were used as positive controls for these assays. Whole cell assays were used for RTK inhibitory activity with the synthesized compounds and controls since these assays afford more meaningful results for translation to in vivo studies. The effect of compounds on cell proliferation was measured using A431 cancer cells, known to overexpress EGFR.³⁴ Cell proliferation was assessed using CYQUANT®, a DNA intercalating dye that has been

shown to give a linear approximation of cell number.³⁵ Finally, the effect of selected compounds on angiogenesis was assessed using the chicken embryo chorioallantoic membrane (CAM) assay, a standard test for angiogenesis.³⁶ Since the IC₅₀ values of RTK inhibitors vary under different assay conditions, we used a standard (control) compound in each of the evaluations (Fig. 4). For EGFR the standards were clinically used agents erlotinib (**2**), sunitinib (**4**) and experimental PD153035 (**25**); for VEGFR-1 the standard was CB676475 (**26**); for VEGFR-2 the standards were clinically used agents erlotinib (**2**), sunitinib (**4**) and semaxanib (**27**); for PDGFR- β the standard was AG1295 (**28**); for the cytotoxicity study against the growth of A431 cells in culture the standard was cisplatin (**29**). Semaxanib (**27**) was also used as the standard for the antiangiogenic CAM assay.

In the EGFR inhibition assay, the most potent compound was **7** (with a *meta*-Br aniline at the 4-position) which was more potent than clinically used erlotinib (**2**) as well as sunitinib (**4**) and was equipotent to the standard EGFR inhibitor PD153035 (**25**). An additional electron withdrawing group such as fluorine at the *para* position on the aniline moiety (**8**) was detrimental for EGFR inhibitory activity. Replacing the *meta*-Br in **8** with a slightly smaller *meta*-Cl in **9** was not conducive for EGFR inhibition either. Compound **10** (with a *meta*-ethynyl aniline at the 4-position like erlotinib) exhibited lower inhibitory activity against EGFR; indicat-

Table 1
Optimization of the Sonogashira coupling reaction



#	Pd source	Ligand	Solvent	Conditions	Yield ^a /Results (%)
1	Pd(PPh ₃) ₄	—	DMF	rt, 72 h	49 ²⁸
2	Pd(PPh ₃) ₄	—	THF	rt, 72 h	No reaction
3	Pd(PPh ₃) ₄	—	MeCN	rt, 72 h	20 ^b
4	Pd(PPh ₃) ₄	—	DMF	100 °C, 24 h	15 ^c
5	Pd(PPh ₃) ₄	—	DMF	μwave, 100 °C, 1 h	25 ^b
6	Pd(PPh ₃) ₄	—	DMF	μwave, 180 °C, 1 h	22 ^c
7	Pd (powder)	PPh ₃	DMF	μwave, 100 °C, 1 h	35
8	Pd (powder)	PPh ₃	DMF	μwave, 150 °C, 1 h	65 ^c
9	Pd (powder)	PPh ₃	DMF	μwave, 150 °C, 10 min	81
10	Pd (powder)	PPh ₃	DMF	μwave, 150 °C, 3.5 min	88
11	Pd(PPh ₃) ₄	—	DMF	μwave, 150 °C, 3.5 min	72

^a Isolated yield.

^b Unreacted starting material was observed on TLC.

^c Considerable amount of baseline spot was observed on TLC. Attempts to analyze this material were not made.

Table 2
IC₅₀ values (μM) for kinase inhibition, A431 cytotoxicity and CAM angiogenesis inhibition assay

Compd	R	EGFR inhibition ^a	VEGFR-1 inhibition ^a	VEGFR-2 inhibition ^a	PDGFR-β inhibition ^a	A431 cytotoxicity ^a	CAM angiogenesis inhibition ^a
2	—	1.2 ± 0.2	—	124.7 ± 18.2	12.2 ± 1.9	—	—
4	—	172.1 ± 19.4	—	18.9 ± 2.7	83.1 ± 10.1	—	—
7	3'-Br	0.3 ± 0.04	>50	49.9 ± 9.8	13.4 ± 3.9	19.6 ± 5.0	7.23 ± 0.9
8	3'-Br, 4'-F	85.9 ± 5.1	93.6 ± 10.2	24.1 ± 3.4	>500	12.2 ± 2.0	0.07 ± 0.005
9	3'-Cl, 4'-F	110.6 ± 0.19	>200	>200	>500	27.0 ± 3.5	11.3 ± 1.9
10	3'-C ₂ H	19.9 ± 2.1	103.1 ± 17.1	43.6 ± 6.1	331.5 ± 48.2	0.9 ± 0.12	13.9 ± 1.4
11	3'-CF ₃	19.3 ± 1.5	>200	16.7 ± 3.1	>500	3.4 ± 0.4	1.09 ± 0.15
12	3'-CF ₃ , 4'-F	15.6 ± 2.3	>200	124.5 ± 21.1	>500	3.2 ± 0.34	14.0 ± 1.5
14	3'-Br, 4'-F	5.4 ± 0.31	>200	>200	89.7 ± 10.2	1.0 ± 0.17	0.9 ± 0.12
15	3'-Cl, 4'-F	16.3 ± 2.8	>200	89.3 ± 9.7	>500	2.6 ± 0.3	2.0 ± 0.31
16	3'-C ₂ H	>200	156.3 ± 18.2	125.6 ± 19.8	430.1 ± 50.1	29.9 ± 3.1	3.2 ± 0.41
17	3'-CF ₃	12.8 ± 1.7	129.6 ± 17.2	16.7 ± 2.5	>500	2.9 ± 0.4	1.6 ± 0.2
18	3'-CF ₃ , 4'-F	26.9 ± 4.1	189.6 ± 23.1	150.9	>500	1.9 ± 0.2	8.6 ± 0.9
25	—	0.23 ± 0.04	—	—	—	12.6 ± 3.1	—
26	—	—	14.1 ± 2.8	—	—	—	—
27	—	—	—	12.0 ± 2.7	—	—	0.085 ± 0.003
28	—	—	—	—	6.2 ± 1.3	—	—
29	—	—	—	—	—	10.6 ± 2.9	—

^a Standard deviation for three experiments.

ing a possible different binding mode. Similarly, substitution of a larger electron withdrawing *meta*-CF₃ group on the 4-anilino moiety in **11** led to diminished EGFR inhibitory activity as compared to **7** and PD153035 (**25**). An additional electron withdrawing fluoro group at the *para*-position in **12** did not improve the IC₅₀ value against EGFR as compared with **11**. The substitution requirement (*meta*-Br) for EGFR inhibition was very subtle. A bulkier or smaller substituent at the *meta*-position on the 4-anilino ring was not conducive for potent EGFR inhibition.

For compounds with a trimethylacetyl group on the 2-amino moiety (**14–18**), EGFR inhibition was improved for **14** (16-fold compared to **8**), **15** (6.5-fold compared to **9**) and **17** (1.4-fold compared to **11**). This improvement may be attributed to the additional interaction of these analogs with hydrophobic site II as hypothesized and/or due to improved cell permeability of the compounds. However, the same trend was not observed for **16** (inactive) and **18** (1.7-fold less active than **12**) in the EGFR inhibitory assay and per-

haps could be attributed to a different mode of binding of **16** and **18**.

Compounds **8**, **10**, **16–18** inhibited VEGFR-1 with IC₅₀ values in the three-digit micromolar range and were about 5- to 11-fold less potent than the standard CB676475 (**26**). The trimethylacetyl group on the 2-amino moiety exhibited a detrimental effect on the inhibitory potency against VEGFR-1 (compare **8** with **14** and **10** with **16**). However this trend was not observed for **11** and **17**.

Against VEGFR-2, compounds **11** and **17** (both with *meta*-CF₃ substitution on the 4-anilino) were the most potent compounds of the series and were much more potent than clinically used erlotinib (**2**) and were equipotent with clinically used sunitinib (**4**) and only 1.5-fold less potent as compared to the standard semaxanib (**27**) that is in clinical trials. In both compounds an additional electron withdrawing fluoro group at the *para*-position of 4-anilino substituent led to an 8- to 9-fold loss of activity (compounds **12** and **18**, respectively), underlining the stringent requirement of

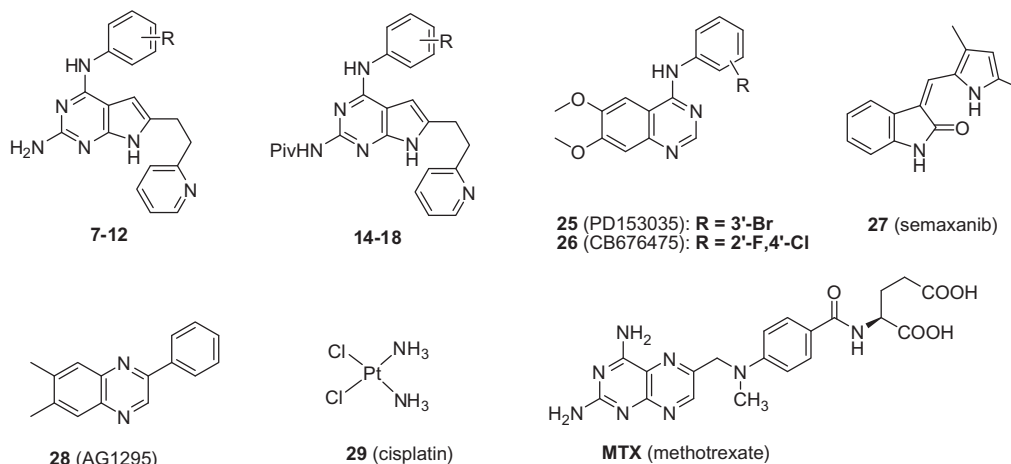


Figure 4. Designed compounds and standard compounds used in the biological assays.

electronics on the 4-anilino substituent for VEGFR-2 inhibitory activity. Compound **7** with a *meta*-Br anilino moiety exhibited two-digit micromolar IC_{50} value and was more potent than erlotinib (**2**) but only about half as potent as sunitinib (**4**) and 4.7-fold less potent than semaxanib (**27**). An additional electron withdrawing fluoro group at the *para*-position of anilino moiety resulted in **8** which afforded a 2-fold improvement in activity and was much more potent than clinically used erlotinib (**2**); about equipotent with sunitinib (**4**) and only 2.4-fold less potent than semaxanib (**27**). Compound **17** with a *meta*-CF₃ group was equipotent with sunitinib (**4**) and somewhat less active compared to semaxanib (**27**). Replacement of the *meta*-Br in **8** to a slightly smaller *meta*-Cl in **9** led to loss of activity. Substitution on the 2-amino group did not affect VEGFR-2 inhibition. A bulkier, electron withdrawing substituent at the *meta*-position on the 4-anilino ring was necessary for potent VEGFR-2 inhibition. Substitution on the 2-amino group did not improve inhibitory activity against VEGFR-2.

Against PDGFR- β , the most potent compound was again **7** (with a *meta*-Br aniline) and was equipotent with erlotinib (**2**) and about 6-fold more potent than sunitinib (**4**) and only about 2-fold less potent than AG1295 (**28**). Additional substitution of a small electron withdrawing fluoro group at the *para*-position on the anilino moiety (in **8**) resulted in significantly diminished inhibition of PDGFR- β . Similarly **9** showed diminished inhibitory activity. Substitution of a *meta*-Br with a larger ethynyl group (in **11**) led to a 25-fold loss of activity. Thus bulky groups at *meta*-position (**11**, **12**) were not tolerated for PDGFR- β inhibitory activity. For PDGFR- β inhibition, substitution on the 2-amino group improved activity for **14** (compared with **8**); and was equipotent as sunitinib (**4**) while for **16** (compared with **10**) activity decreased.

Most of the compounds in this series exhibited good potency in the A431 cytotoxicity assay compared to the standard cisplatin (**29**). Compound **7** showed cytotoxicity against A431 cells at IC_{50} of 19.6 μ M. Substitution of an electron withdrawing fluoro group led to 1.6-fold improvement in cytotoxicity. Substitution of *meta*-Br with slightly smaller chloro group resulted in about 2.2-fold loss of activity. Compound **10** (*meta*-ethynyl) was the most potent compound in A431 cytotoxicity assay, and was 8-fold more potent than cisplatin (**29**). Substitution at the 2-amino group improved cytotoxicity in most cases (**14**, **15**, **17** and **18**) except one (**16**). Activity of **14** against EGFR appears to be translated into A431 cytotoxicity. Overall, compounds with bulkier substituents at the *meta*-position of the 4-anilino ring exhibited improved cytotoxicity against A431 cells.

In the CAM angiogenesis assay compound **8** was the most potent compound and was 1.2-fold better than semaxanib (**27**). Com-

pound **14** was only 10-fold less potent than semaxanib (**27**). In addition compounds **11** and **15–18** exhibited IC_{50} values in the one-digit micromolar range in the CAM angiogenesis assay. In most cases the trimethylacetyl group on the 2-amino moiety improved CAM inhibition (except for **14** and **17**). Compounds exhibiting potent inhibition of angiogenesis (**8**, **11**, **14** and **17**) have shown inhibition of at least two RTKs.

From this study compound **8**, was found to be a potent inhibitor of angiogenesis (IC_{50} = 0.07 μ M in the CAM angiogenesis inhibition assay) and it also inhibited VEGFR-2, EGFR and VEGFR-1. Though the potency of **8** against these three RTKs was not the best (as compared to the corresponding standards used), the overall effect of simultaneous inhibition of three RTKs may account for the potent inhibition of angiogenesis (CAM assay). In general, from this in vitro study, compounds that exhibit relatively good inhibition of angiogenesis (CAM assay) also exhibited inhibition of at least two of the RTKs evaluated. This underscores the fact that angiogenesis is a multifaceted, multicellular, multikinase, and multiprotein activated process and that perhaps RTKs other than those evaluated, may also be inhibited, providing a synergistic effect on the overall angiogenesis process.

On the basis of the in vitro activity of compound **8** it was selected for in vivo evaluation in a mouse tumor model in order to determine its effect on tumor growth rates, metastasis, and tumor angiogenesis.

2.4. In vivo evaluation of compound **8** in a B16-F10 syngeneic tumor model

To examine whether compound **8** was effective in vivo in reducing tumor volume and metastasis, a syngeneic mouse tumor model was used. This model is a widely accepted model for testing tumor growth and metastases.³⁷ The B16 model of tumor growth produces almost quantitative (100%) tumor take in a very short time after administration,^{38,39} so animals are not wasted. The B16 tumor cells are skin-derived, so subcutaneous implantation is adequate and resulting tumors are superficial, and easily measured. The B16-F10 variant used in these studies is highly metastatic, and most if not all metastases go to the lung, making metastasis evaluation very facile.^{38–41} Unlike most human tumor xenograft models, the B16 model produces highly vascularized tumors so that the effect of tumor-mediated angiogenesis can be evaluated.^{38–41}

The maximal tolerated dose for **8** was 12.5 mg/kg twice weekly as determined in the whole animal toxicity assay (Section 4). This same dose was used for the in vivo evaluation. Compound **8** was injected intraperitoneally (IP) every Monday (AM) and Thursday

(PM) at 12.5 mg/kg dose and was compared with the antifolate methotrexate (MTX) injected IP at 10 mg/kg. Tumor volume was calculated using the formula length \times width \times depth. Tumor growth rate was calculated using a linear regression analysis algorithm using the software GraphPad Prism 4.0.c. At the experiment's end, animals were humanly euthanized using carbon dioxide, tumors and lungs excised, fixed in 20% neutral buffered formalin for 8–10 h, embedded into paraffin, and hematoxylin–eosin (H&E) stain of three separate tissue sections completed to span the tumor/lung. Metastases per lung lobe counted using the H&E stained sections. Blood vessels per unit area were counted in 5 fields at 100 \times magnification and averaged. Tumor growth rates were compared statistically using two-way ANOVA with a Repeated Measures post-test and tumor vascularity and metastases were compared using one-way ANOVA and a Neuman–Keuls post test with the null hypothesis rejected when $P < 0.05$.

The results of compound **8** on the B16-F10 syngeneic tumor model are shown in Figure 5A–D.

It was found that **8** at 12.5 mg/kg given twice weekly resulted in a significant decrease in B16-F10 tumor growth rate as compared to solvent treated animals (Fig. 5A). On the other hand, MTX at 10 mg/kg given twice weekly was slightly better at inhibiting primary tumor growth as compared to **8**.

There was also significantly less increase in tumor volume (Fig. 5B) in animals treated with compound **8** or MTX as compared to untreated animals. Compound **8** (12.5 mg/Kg twice weekly dose) was as effective as MTX (10 mg/kg twice weekly dose) in preventing increase in tumor volume over the entire course of the experiment (Fig. 5B).

With respect to the effect of these agents on the vascular density (Fig. 5C) of the resulting tumors, compound **8** led to slightly more vessels per unit area as compared to treatment with MTX.

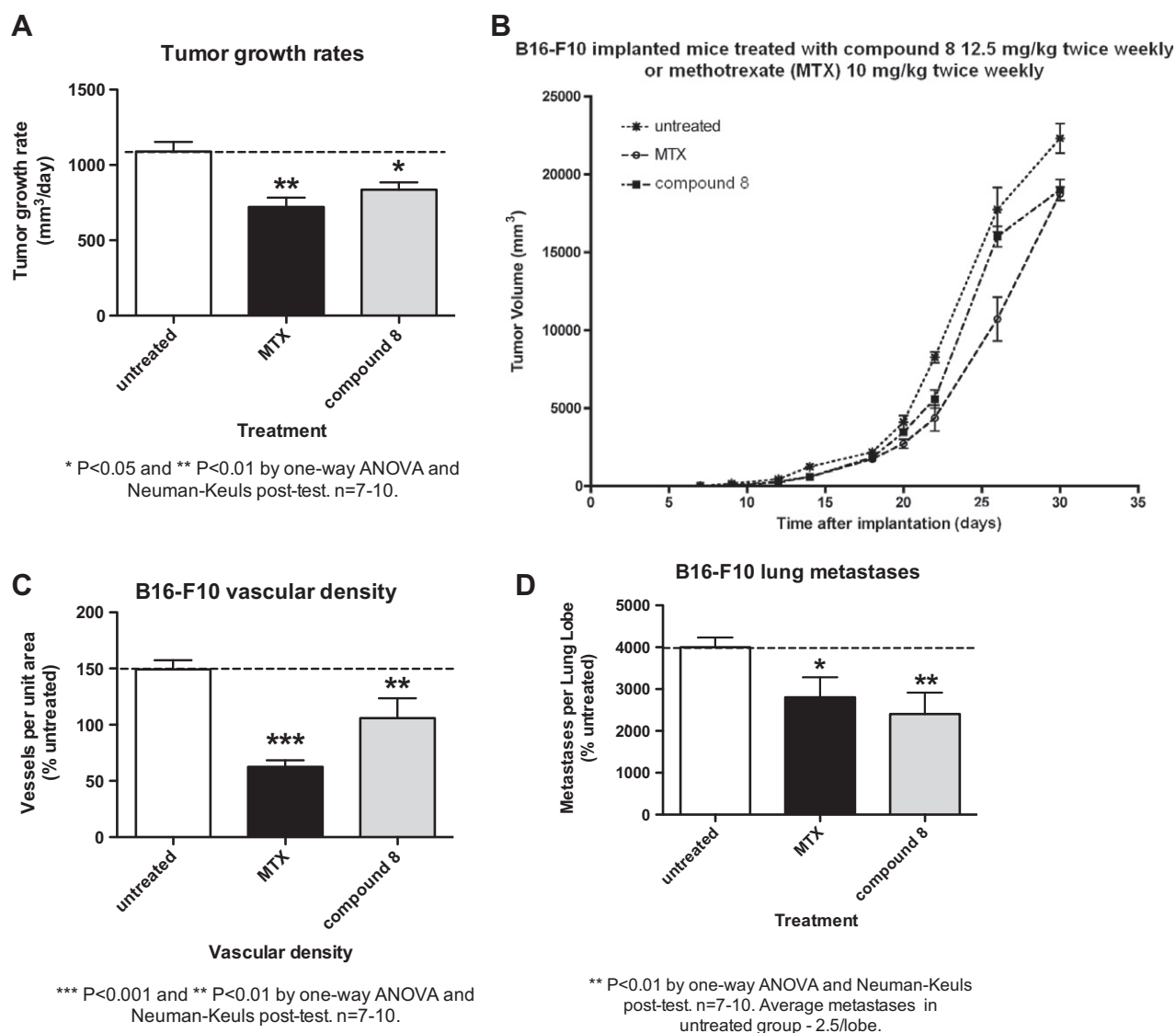


Figure 5. (A) Effect of compound **8** and MTX on the growth of B16-F10 primary tumors. Mice bearing B16-F10 GFP-tagged tumors were treated biweekly with 12.5 mg/kg of compound **8** or 10 mg/kg of MTX and tumors measured biweekly. Tumor growth rates were calculated using linear regression analysis in GraphPad Prism 4.0 software. * $P < 0.05$, ** $P < 0.01$ as compared to untreated animals; using two-way ANOVA with Repeated Measures post-test, $n = 7-10$. (B) Effect of compound **8** and MTX on the tumor volume (mm³) of B16-F10 primary tumors. Mice bearing B16-F10 GFP-tagged tumors were treated biweekly with 12.5 mg/kg of compound **8** or 10 mg/kg of MTX and tumors measured biweekly. Tumor volume was calculated using the formula length \times width \times depth. (C) Effect of compound **8** and MTX on the vascular density of B16-F10 primary tumors. Blood vessels per unit area were counted in 5 fields at 100 \times magnification and averaged. *** $P < 0.001$, ** $P < 0.01$ as compared to untreated animals; using one-way ANOVA and Neuman-Keuls post-test, $n = 7-10$. (D) Effect of compound **8** and MTX on B16-F10 lung metastases. Metastases per lung lobe counted using the H&E stained sections. ** $P < 0.01$ as compared to untreated animals; using one-way ANOVA and Neuman-Keuls post-test, $n = 7-10$. Average metastases in untreated group ~ 2.5 /lobe.

However this decrease in vascular density of B16-F10 tumors by compound **8** (as well as MTX) was statistically significant as compared to solvent treated (untreated) animals. These results support the antiangiogenic activity of compound **8**.

Treatment with **8** also resulted in significantly decreased numbers of B16-F10 lung metastases (Fig. 5D) as compared to treatment with MTX and untreated control.

Compound **8** exhibited excellent activity in the in vivo antitumor evaluation, compared to MTX. This could be the result of a synergistic effect of multiple RTK inhibition. Decrease in number of lung metastases along with a decrease in vascular density of tumor in animals treated with **8** corroborates our hypothesis.

3. Summary

In summary six novel N^4 -phenylsubstituted-6-(2-pyridin-2-ylethyl)-7H-pyrrolo[2,3-d]pyrimidine-2,4-diamines and their N^2 -trimethylacetyl substituted intermediate analogs were synthesized using a microwave-assisted Sonogashira reaction as a key step. The optimized microwave-mediated reaction resulted in considerably higher yields compared to the previously described bench-top reaction. These compounds were evaluated in cell-based assay for their inhibitory activity against EGFR, VEGFR-1, VEGFR-2, and PDGFR- β . Minor variations in the substitution on the 4-anilino ring led to significant differences in inhibition of the various RTKs. In addition, in some cases, the substitution on the 2-amino group resulted in improved inhibitory activity against particular RTKs. However this trend was not observed in all cases. These variations in activity could be attributed to the stringent requirements for binding in individual RTKs and/or due to differences in cell permeability of these compounds. Compound **8** was evaluated in vivo at 12.5 mg/kg dose in B16-F10 syngeneic mouse tumor model. In this study a significant reduction in tumor growth rate, in tumor vascular density and in metastases of the primary tumor to the lung was observed for compound **8**.

4. Experimental

4.1. General methods for synthesis

All evaporations were carried out in vacuo with a rotary evaporator. Analytical samples were dried in vacuo (0.2 mm Hg) in a CHEM-DRY drying apparatus over P_2O_5 at 70 °C. Melting points were determined on a MEL-TEMP II melting point apparatus with FLUKE 51 K/J electronic thermometer and are uncorrected. Nuclear magnetic resonance spectra for proton (1H NMR) were recorded on a Bruker WH-300 (300 MHz) spectrometer. The chemical shift values are expressed in ppm (parts per million) relative to tetramethylsilane as an internal standard: s, singlet; d, doublet; t, triplet; q, quartet; m, multiplet; br, broad singlet. The relative integrals of peak areas agreed with those expected for the assigned structures. Thin-layer chromatography (TLC) was performed on WHATMAN UV254 silica gel plates with a fluorescent indicator, and the spots were visualized under 254 and/or 365 nm illumination. Proportions of solvents used for TLC are by volume. Column chromatography was performed on a 230–400 mesh silica gel purchased from Fisher Scientific. Elemental analyses were performed by Atlantic Microlab, Inc., Norcross, GA. The results of elemental analyses for the compounds that were biologically evaluated were in agreement with calculated values within $\pm 0.4\%$ range. Fractional moles of water or organic solvents sometimes found in some analytical samples could not be prevented in spite of 24–48 h of drying in vacuo and were confirmed where possible by their presence in the 1H NMR spectra. All solvents and chemicals were purchased from Aldrich Chemical Co. or Thermo Fisher Scientific and were used as received.

4.2. 2,2-Dimethyl-N-[4-oxo-6-(pyridin-2-ylethynyl)-4,7-dihydro-3H-pyrrolo[2,3-d]pyrimidin-2-yl]propanamide (**21**)³¹

To a 5 mL microwave vial were added **19**³¹ (100 mg, 0.28 mmol), 2-ethynylpyridine **20** (30 mg, 0.29 mmol), palladium (14 mg, 0.13 mmol), CuI (10 mg, 0.05 mmol), triphenyl phosphine (53.2 mg, 0.2 mmol) followed by the addition of DMF (4 mL) and triethylamine (0.5 mL). The mixture was irradiated in a Smith Creator (personal chemistry) microwaves or a Initiator (Biotage) microwave for 3.5 min at 150 °C. Silica gel (500 mg) was added to the mixture and the solvents were removed under reduced pressure to obtain a silica gel plug which was loaded on a silica gel column (2.5 cm \times 15 cm) and chromatographed with 1.5% MeOH in $CHCl_3$. Fractions containing the product (TLC) were pooled and evaporated to afford **21** (83 mg, 88%) as a pale yellow solid: TLC R_f 0.25 (MeOH/ $CHCl_3$, 1:19); mp >270 °C dec. (lit.³¹ mp >270 °C dec.); 1H NMR (300 MHz) (DMSO- d_6) δ 1.24 (s, 9H, C(CH₃)₃), 6.89 (s, 1H, C5-H), 7.43 (d, 1H, $J = 4.8$ Hz, C₅H₄N), 7.61 (d, 1H, $J = 4.8$ Hz, C₅H₄N), 7.86 (t, 1H, $J = 4.8$ Hz, C₅H₄N), 8.61 (br, 1H, C₅H₄N), 10.99 (s, 1H, 2-NHPiv, exch), 11.97 (br, 1H, 3-NH, exch), 12.36 (br, 1H, 7-NH, exch).

4.3. 2,2-Dimethyl-N-[4-oxo-6-(2-pyridin-2-ylethyl)-4,7-dihydro-3H-pyrrolo[2,3-d]pyrimidin-2-yl]propanamide (**22**)³¹

To a Parr hydrogenation bottle was added 5% Pd/C (200 mg) followed by **21** (200 mg, 0.59 mmol) dissolved in a mixture of DMF and THF (1:5) (24 mL) and 2–3 drops of concd ammonium hydroxide. The reaction mixture was shaken under 50 psi hydrogen pressure for 24 h. At the end of the reaction, the slurry was filtered through a celite pad which was washed with hot THF-DMF (25 mL \times 2). The filtrate was concentrated under reduced pressure. Silica gel (1 g) was added and the solvent was evaporated to form a plug which was loaded on top of a silica gel column (2.5 \times 10 cm) and eluted with 1.5% MeOH in $CHCl_3$. Fractions containing the product (TLC) were pooled and evaporated to afford **22** (161 mg, 75%) as an off-white solid: R_f 0.20 (MeOH/ $CHCl_3$, 1:19); mp 216.5–217.8 °C (lit.³¹ mp 217–218 °C) 1H NMR (300 MHz) (DMSO- d_6): δ 1.24 (s, 9H, C(CH₃)₃), 3.01–3.05 (m, 4H, CH₂CH₂), 6.08 (s, 1H, C5-H), 7.19–7.23 (m, 1H, C₅H₄N), 7.27 (d, 1H, $J = 4.8$ Hz, C₅H₄N), 7.68 (t, 1H, $J = 4.8$ Hz, C₅H₄N), 7.27 (d, 1H, $J = 4.8$ Hz, C₅H₄N), 10.76 (br, 1H, 2-NHPiv, exch), 11.45 (br, 1H, 3-NH, exch), 11.79 (br, 1H, 7-NH, exch).

4.4. N-[4-chloro-6-(2-pyridin-2-ylethyl)-7H-pyrrolo[2,3-d]pyrimidin-2-yl]-2,2-dimethylpropanamide (**23**)

To a round-bottom flask was added **22** (300 mg, 0.96 mmol; pre-dried over phosphorous pentoxide using high vacuum for 8 h) and phosphorous oxychloride (10 mL). The slurry was heated to form a light brown solution. Reaction was continued at reflux for 3 h; at the end of which, the mixture was allowed to cool to room temperature. Unreacted phosphorous oxychloride was removed under reduced pressure to afford a gummy residue. Trituration of this residue with ice-water (approx 50 ml); followed by the addition of concd NH_4OH to adjust the pH to 4. The light brown precipitate thus formed was filtered, air-dried and then dissolved in $CHCl_3$ -MeOH (1:1, 50 mL). Silica gel (1 g) was added and solvents evaporated to form a silica gel plug which was loaded on top of silica gel column (2.5 \times 15 cm) and eluted with 1% MeOH in $CHCl_3$. Fractions containing the product (TLC) were pooled and evaporated under reduced pressure to afford **23** (240 mg, 70%) as a white solid: TLC R_f 0.3 (MeOH/ $CHCl_3$, 1:19); mp 157–158.5 °C; 1H NMR (300 MHz) (DMSO- d_6): δ 1.22 (s, 9H, C(CH₃)₃), 3.16 (s, 4H, -CH₂-CH₂-), 6.22 (s, 1H, C5-CH), 7.25–7.28 (m, 1H, C₅H₄N), 7.29 (d, 1H, $J = 5.1$ Hz, C₅H₄N), 7.96 (t, 1H, $J = 4.8$ Hz, C₅H₄N), 8.51

(d, 1H, $J = 4.8$ Hz, C_5H_4N), 9.97 (s, 1H, 2-NHPiv, exch), 12.30 (s, 1H, 7-NH, exch). HRMS (EI) calcd for $C_{18}H_{20}ClN_5O$: 357.1356, found 357.1392.

4.5. General procedure for the synthesis of compounds 13–18

To a round-bottom flask was added **23** and the appropriate substituted anilines **24a–e** in isopropanol (10 mL), followed by the addition of two drops of concd HCl. The reaction was continued at reflux for 3 h at the end of which the solvent was evaporated under reduced pressure. The residue was dissolved in methanol (10 mL), and silica gel (1 g) was added to the solution which was then evaporated to dryness to form a plug. The silica gel plug obtained was loaded onto a silica gel column and eluted with 1.5% methanol in chloroform. Fractions corresponding to the product (TLC) were pooled and evaporated to dryness under reduced pressure to afford the product.

4.5.1. *N*-{4-[(3-Bromophenyl)amino]-6-(2-pyridin-2-yl-ethyl)-7H-pyrrolo[2,3-*d*]pyrimidin-2-yl}-2,2-dimethylpropanamide (**13**)

Reaction of **20** (80 mg, 0.24 mmol) and 3-bromoaniline **21a** (160 mg, 0.96 mmol), using the general procedure described above, gave **13** (110 mg; 98%) as yellow foam: TLC R_f 0.15 (MeOH/CHCl₃, 1:19); ¹H NMR (300 MHz) (DMSO-*d*₆): δ 1.24 (s, 9H, C(CH₃)₃), 3.07–3.19 (m, 4H, –CH₂CH₂–), 6.43 (s, 1H, C5–CH), 7.08–7.27 (m, 5H, ArH), 7.66–7.71 (m, 1H, ArH), 8.02 (d, 1H, $J = 8.0$ Hz, ArH), 8.50 (d, 1H, $J = 4.9$ Hz, ArH), 9.29 (s, 1H, 2-NHPiv or 4-NH, exch), 9.38 (s, 1H, 2-NHPiv or 4-NH, exch), 11.51 (s, 1H, 7-NH, exch); HRMS (EI) calcd for $C_{24}H_{25}N_6BrO$: 492.1273, found 492.1275.

4.5.2. *N*-{4-[(3-Bromo,4-fluorophenyl)amino]-6-(2-pyridin-2-yl-ethyl)-7H-pyrrolo[2,3-*d*]pyrimidin-2-yl}the-2,2-dimethylpropanamide (**14**)

Reaction of **20** (143 mg, 0.4 mmol) and 3-bromo, 4-fluoroaniline **21b** (300 mg, 1.6 mmol), using a general procedure described above, gave **14** (200 mg; 96%) as off-white fluffy crystals: TLC R_f 0.49 (MeOH/CHCl₃, 1:10); mp 149.5–151.5 °C; ¹H NMR (300 MHz) (DMSO-*d*₆): δ 1.24 (s, 9H, C(CH₃)₃), 3.14 (t, 2H, $J = 6.3$ Hz, –CH₂–), 3.26 (t, 2H, $J = 6.3$ Hz, –CH₂–), 6.40 (s, 1H, C5–CH), 7.25–7.27 (m, 3H, ArH), 7.69 (s, 1H, ArH), 7.98 (br, 1H, ArH), 8.52 (d, 1H, $J = 7.4$ Hz, ArH), 8.72 (br, 1H, ArH), 9.31 (s, 1H, 4-NH or 2-NHPiv, exch), 9.39 (s, 1H, 2-NHPiv or 4-NH, exch), 11.49 (s, 1H, 7-NH, exch). Anal. (C₂₄H₂₄N₆BrFO) CHNBrF.

4.5.3. *N*-{4-[(3-Chloro,4-fluorophenyl)amino]-6-(2-pyridin-2-yl-ethyl)-7H-pyrrolo[2,3-*d*]pyrimidin-2-yl}-2,2-dimethylpropanamide (**15**)

Reaction of **20** (143 mg, 0.4 mmol) and 3-chloro,4-fluoroaniline **21c** (235 mg, 1.6 mmol), using the general procedure described above, afforded **15** (150 g; 80%) as a white fluffy solid: TLC R_f 0.5 (MeOH/CHCl₃, 1:10); mp 157–159 °C; ¹H NMR (300 MHz) (DMSO-*d*₆): δ 1.24 (s, 9H, C(CH₃)₃), 3.13 (t, 2H, $J = 6.0$ Hz, –CH₂–), 3.27 (t, 2H, $J = 6.0$ Hz, –CH₂–), 6.40 (s, 1H, C5–CH), 7.27–7.29 (m, 3H, ArH), 7.68 (s, 1H, ArH), 7.95 (br, 1H, ArH), 8.47 (d, 1H, $J = 7.8$ Hz, ArH), 8.66 (d, 1H, $J = 4.8$ Hz, ArH), 9.31 (s, 1H, 4-NH or 2-NHPiv, exch), 9.39 (s, 1H, 2-NHPiv or 4-NH, exch), 11.50 (s, 1H, 7-NH, exch). HRMS (EI) calcd for $C_{24}H_{24}N_6ClFO$: 466.1678, found 466.1684.

4.5.4. *N*-{4-[(3-Ethynylphenyl)amino]-6-(2-pyridin-2-yl-ethyl)-7H-pyrrolo[2,3-*d*]pyrimidin-2-yl}-2,2-dimethylpropanamide (**16**)

Reaction of **20** (125 mg, 0.35 mmol) and 3-ethynylaniline **21d** (164 mg, 1.4 mmol), using the general procedure described above,

gave **16** (130 mg; 85%) as a off-white solid: TLC R_f 0.46 (MeOH/CHCl₃, 1:10); mp 120–125 °C; ¹H NMR (300 MHz) (DMSO-*d*₆): δ 1.23 (s, 9H, C(CH₃)₃), 3.12–3.14 (m, 4H, –CH₂CH₂–), 4.10 (s, 1H, C₂H), 6.42 (s, 1H, C5–CH), 7.24–7.28 (m, 3H, ArH), 7.69 (t, 1H, $J = 6.0$ Hz, ArH), 8.12 (s, 1H, ArH), 8.24 (d, 1H, $J = 6.0$ Hz, ArH), 8.51 (s, 1H, ArH), 9.22 (s, 1H, 2-NHPiv or 4-NH, exch), 9.36 (s, 1H, 2-NHPiv or 4-NH, exch), 11.51 (br, 1H, 7-NH, exch); HRMS (ESI) calcd for $C_{26}H_{27}N_6O$ (M+H)⁺: 439.2267, found 439.2246.

4.5.5. *N*-{4-[(3-Trifluoromethylphenyl)amino]-6-(2-pyridin-2-yl-ethyl)-7H-pyrrolo[2,3-*d*]pyrimidin-2-yl}-2,2-dimethylpropanamide (**17**)

Reaction of **20** (125 mg, 0.35 mmol) and 3-trifluoromethylaniline **21e** (225 mg, 1.4 mmol), using the general procedure described above, gave **17** (151 mg; 89%) as a white fluffy solid: TLC R_f 0.47 (MeOH/CHCl₃, 1:10); mp 155.9–158.2 °C; ¹H NMR (300 MHz) (DMSO-*d*₆): δ 1.24 (s, 9H, C(CH₃)₃), 3.13–3.16 (m, 4H, –CH₂CH₂–), 6.45 (s, 1H, C5–CH), 7.23–7.26 (m, 3H, ArH), 7.49 (t, 1H, $J = 7.2$ Hz, ArH), 7.69 (t, 1H, $J = 7.2$ Hz, ArH), 8.30 (d, 1H, $J = 7.2$ Hz, ArH), 8.51 (s, 1H, ArH), 8.65 (s, 1H, ArH), 9.42 (s, 1H, 2-NHPiv or 4-NH, exch), 9.48 (s, 1H, 2-NHPiv or 4-NH, exch), 11.55 (br, 1H, 7-NH, exch). Anal. (C₂₅H₂₅N₆F₃O 0.3H₂O) CHNF.

4.5.6. *N*-{4-[(3-Trifluoromethyl,4-fluorophenyl)amino]-6-(2-pyridin-2-yl-ethyl)-7H-pyrrolo[2,3-*d*]pyrimidin-2-yl}-2,2-dimethylpropanamide (**18**)

Reaction of **20** (150 mg, 0.42 mmol) and 4-fluoro-3-trifluoromethylaniline **21f** (300 mg, 1.67 mmol), using the general procedure described above, gave **18** (200 mg; 95%) as a white fluffy solid: TLC R_f 0.46 (MeOH/CHCl₃, 1:10); mp 167.5–169 °C; ¹H NMR (300 MHz) (DMSO-*d*₆): δ 1.23 (s, 9H, C(CH₃)₃), 3.13–3.15 (m, 4H, –CH₂CH₂–), 6.41 (s, 1H, C5–CH), 7.21–7.24 (m, 2H, ArH), 7.39 (t, 1H, $J = 7.5$ Hz, ArH), 7.69 (t, 1H, $J = 7.5$ Hz, ArH), 8.34 (br, 1H, ArH), 8.51 (d, 1H, $J = 4.2$ Hz, ArH), 8.67 (d, 1H, $J = 5.4$ Hz, ArH), 9.41 (s, 1H, 2-NHPiv or 4-NH, exch), 9.48 (s, 1H, 2-NHPiv or 4-NH, exch), 11.53 (s, 1H, 7-NH, exch). Anal. (C₂₅H₂₄N₆F₄O 0.8H₂O) CHNF.

4.6. General procedure for the synthesis of compounds 7–12

To a round-bottom flask was added **13–18** in methanol (10 mL), followed by the addition of 1 N NaOH (2 mL). The reaction was completed after heating at 70 °C for 10 h. Methanol was evaporated under reduced pressure to afford a residue, which was filtered, washed with water (10 mL) and air-dried. The residue was dissolved in methanol (10 mL), and silica gel (1 g) was added to the solution which was then evaporated to dryness to form a plug. The silica gel plug thus obtained was loaded on top of a silica gel column (1.5 × 15 cm) and eluted with 1.5% methanol in chloroform. Fractions corresponding to the product (TLC) were pooled and evaporated to dryness under reduced pressure to afford the product.

4.6.1. *N*⁴-(3-Bromophenyl)-6-(2-pyridin-2-yl-ethyl)-7H-pyrrolo[2,3-*d*]pyrimidine-2,4-diamine (**7**)

Compound **7** was obtained from **13** (0.09 g, 0.19 mmol) using the general procedure described above to afford after purification 40 mg (54%) as a pale yellow solid: TLC R_f 0.31 (MeOH/CHCl₃, 1:9); mp 200–202 °C; ¹H NMR (300 MHz) (DMSO-*d*₆): δ 2.97–3.01 (m, 4H, –CH₂CH₂–), 5.83 (s, 2H, 2-NH₂, exch), 6.24 (s, 1H, C5–CH), 7.08–7.28 (m, 4H, ArH), 7.69 (br, 1H, ArH), 8.00 (d, 1H, $J = 8.0$ Hz, ArH), 8.11 (m, 1H, ArH), 8.50 (d, 1H, $J = 4.8$ Hz, ArH), 8.97 (s, 1H, 4-NH, exch), 10.96 (s, 1H, 7-NH, exch). HRMS (EI) calcd for $C_{19}H_{17}N_5Br$: 408.0698, found 408.0684.

4.6.2. *N*⁴-(3-Bromo,4-fluorophenyl)-6-(2-pyridin-2-yl-ethyl)-7*H*-pyrrolo[2,3-*d*]pyrimidine-2,4-diamine (8)

Compound **8** was obtained from **14** (130 mg, 0.25 mmol) using the general procedure described above to afford a gummy residue which was stirred with hexanes and filtered to obtain 65 mg (61%) of **8** as a off-white solid: TLC *R*_f 0.23 (MeOH/CHCl₃, 1:10); mp 223–226 °C; ¹H NMR (300 MHz) (DMSO-*d*₆): δ 3.00 (t, 2H, *J* = 6.9 Hz, –CH₂–), 3.15 (t, 2H, *J* = 6.9 Hz, –CH₂–), 5.74 (br, 2H, 2-NH₂, exch), 6.19 (s, 1H, C5–CH), 7.21–7.24 (m, 3H, ArH), 7.69 (t, 1H, *J* = 7.2 Hz, ArH), 7.85 (br, 1H, ArH), 8.22 (d, 1H, *J* = 6.3 Hz, ArH), 8.49 (s, 1H, ArH), 8.90 (s, 1H, 4-NH, exch), 10.89 (br, 1H, 7-NH, exch). Anal. (C₁₉H₁₆N₆BrF: 0.1 C₆H₁₄) CHNBr. HRMS (EI) calcd for C₁₉H₁₆N₆BrF: 426.0598, found 426.0603.

4.6.3. *N*⁴-(3-Chloro,4-fluorophenyl)-6-(2-pyridin-2-yl-ethyl)-7*H*-pyrrolo[2,3-*d*]pyrimidine-2,4-diamine (9)

Compound **9** was obtained from **15** (100 mg, 0.21 mmol) using the general procedure described above to afford after purification 51 mg (62%) as a light brown solid: TLC *R*_f 0.25 (MeOH/CHCl₃, 1:10); mp >200 °C (decomposed); ¹H NMR (300 MHz) (DMSO-*d*₆): δ 3.07 (t, 2H, *J* = 6.9 Hz, –CH₂–), 3.20 (t, 2H, *J* = 6.9 Hz, –CH₂–), 5.74 (br, 2H, 2-NH₂, exch), 6.19 (s, 1H, C5–CH), 7.23 (m, 3H, ArH), 7.69 (t, 1H, *J* = 7.2 Hz, ArH), 7.85 (br, 1H, ArH), 8.22 (d, 1H, *J* = 6.3 Hz, ArH), 8.49 (s, 1H, ArH), 8.91 (s, 1H, 4-NH, exch), 10.88 (s, 1H, 7-NH, exch). Anal. (C₁₉H₁₆N₆ClF) CHNClF.

4.6.4. *N*⁴-(3-Ethynylphenyl)-6-(2-pyridin-2-yl-ethyl)-7*H*-pyrrolo[2,3-*d*]pyrimidine-2,4-diamine (10)

Compound **10** was obtained from **16** (100 mg, 0.23 mmol) using the general procedure described above to afford after purification 70 mg (86%) as a off-white solid: TLC *R*_f 0.2 (MeOH/CHCl₃, 1:10); mp 229.5–231.5 °C; ¹H NMR (300 MHz) (DMSO-*d*₆): δ 2.98 (t, 2H, *J* = 6.9 Hz, –CH₂–), 3.09 (t, 2H, *J* = 6.9 Hz, –CH₂–), 4.12 (s, 1H, C₂H), 5.68 (br, 2H, 2-NH₂, exch), 6.22 (s, 1H, C5–CH), 7.01 (d, 1H, *J* = 7.5 Hz, ArH), 7.20–7.23 (m, 3H, ArH), 7.68 (t, 1H, *J* = 7.4 Hz, ArH), 7.92 (s, 1H, ArH), 8.08 (d, 1H, *J* = 8.1 Hz, ArH), 8.50 (d, 1H, *J* = 3.5 Hz, ArH), 8.81 (s, 1H, 4-NH, exch), 10.86 (br, 1H, 7-NH, exch). Anal. (C₂₁H₁₈N₆) CHN.

4.6.5. *N*⁴-(3-Trifluoromethylphenyl)-6-(2-pyridin-2-yl-ethyl)-7*H*-pyrrolo[2,3-*d*]pyrimidine-2,4-diamine (11)

Compound **11** was obtained from **17** (125 mg, 0.26 mmol) using the general procedure described above to afford after purification 85 mg (84%) as a light yellow solid: TLC *R*_f 0.19 (MeOH/CHCl₃, 1:10); mp 226.5–227.6 °C; ¹H NMR (300 MHz) (DMSO-*d*₆): δ 3.00 (t, 2H, *J* = 6.1 Hz, –CH₂–), 3.09 (t, 2H, *J* = 6.1 Hz, –CH₂–), 5.73 (br, 2H, 2-NH₂, exch), 6.24 (s, 1H, C5–CH), 7.22–7.25 (m, 3H, ArH), 7.47 (t, 1H, *J* = 7.4 Hz, ArH), 7.67 (d, 1H, *J* = 6.7 Hz, ArH), 8.15 (s, 1H, ArH), 8.44 (d, 1H, *J* = 7.8 Hz, ArH), 8.50 (s, 1H, ArH), 9.08 (s, 1H, 4-NH, exch), 10.92 (br, 1H, 7-NH, exch). Anal. (C₂₀H₁₇N₆F₃) CHNF.

4.6.6. *N*⁴-(3-Trifluoromethyl,4-fluorophenyl)-6-(2-pyridin-2-yl-ethyl)-7*H*-pyrrolo[2,3-*d*]pyrimidine-2,4-diamine (12)

Compound **12** was obtained from **18** (100 mg, 0.2 mmol) using the general procedure described above to afford after purification 65 mg (78%) as a white lustrous crystals: TLC *R*_f 0.26 (MeOH/CHCl₃, 1:10); mp 233.8–234.7 °C; ¹H NMR (300 MHz) (DMSO-*d*₆): δ 3.00 (t, 2H, *J* = 6.6 Hz, –CH₂–), 3.09 (t, 2H, *J* = 6.6 Hz, –CH₂–), 5.70 (br, 2H, 2-NH₂, exch), 6.19 (s, 1H, C5–CH), 7.22–7.24 (m, 2H, ArH), 7.37 (t, 1H, *J* = 7.8 Hz, ArH), 7.68 (t, 1H, *J* = 7.7 Hz, ArH), 8.19 (s, 1H, ArH), 8.44 (d, 1H, *J* = 4.5 Hz, ArH), 8.50 (s, 1H, ArH), 9.07 (s, 1H, 4-NH, exch), 10.90 (br, 1H, 7-NH, exch). Anal. (C₂₀H₁₆N₆F₄·0.2H₂O) CHNF.

4.7. General methods for biological evaluation

4.7.1. Cells

All cells were maintained at 37 °C in a humidified environment containing 5% CO₂ using media from Mediatech (Hemden, NJ). A-431 cells were from the American Type Tissue Collection (Manassas, VA).

4.7.2. Chemicals

All growth factors (bFGF, VEGF, EGF, and PDGF-β) were purchased from Peprotech (Rocky Hill, NJ). PD153035 (**25**), CB676475 (**26**), semaxanib (**27**), AG1295 (**28**), and cisplatin (**29**) were purchased from Calbiochem (San Diego, CA). The CYQUANT cells proliferation assay was from Molecular Probes (Eugene, OR). All other chemicals were from Sigma Chemical Co. unless otherwise noted.

4.7.3. Antibodies

The PY-HRP antibody was from BD Transduction Laboratories (Franklin Lakes, NJ). Antibodies against EGFR, PDGFR-β, FGFR-1, Flk-1, and Flt-1 were purchased from Upstate Biotech (Framingham, MA).

4.7.4. Phosphotyrosine ELISA

Cells used were tumor cell lines naturally expressing high levels of EGFR (A431), Flk-1 (U251), Flt-1 (A498), and PDGFR-β (SF-539). Expression levels at the RNA level were derived from the NCI Developmental Therapeutics Program (NCI-DTP) web site public molecular target information (http://www.dtp.nci.nih.gov/mtargets/mt_index.html). Briefly, cells at 60–75% confluence are placed in serum-free medium for 18 h to reduce the background of phosphorylation. Cells were always >98% viable by Trypan blue exclusion. Cells are then pretreated for 60 min with 10, 3.33, 1.11, 0.37, and 0.12 μM compound followed by 100 ng/ml EGF, VEGF, PDGF-BB, or bFGF for 10 min. The reaction is stopped and cells permeabilized by quickly removing the media from the cells and adding ice-cold Tris-buffered saline (TBS) containing 0.05% Triton X-100, protease inhibitor cocktail and tyrosine phosphatase inhibitor cocktail. The TBS solution is then removed and cells fixed to the plate for 30 min at 60 °C and further incubation in 70% ethanol for an additional 30 min. Cells are further exposed to block (TBS with 1% BSA) for 1 h, washed, and then a horseradish peroxidase (HRP)-conjugated phosphotyrosine (PY) antibody added overnight. The antibody is removed, cells are washed again in TBS, exposed to an enhanced luminal ELISA substrate (Pierce Chemical, Rockford, IL) and light emission measured using a UV products (Upland, CA) BioChemi digital darkroom. Data were graphed as a percent of cells receiving growth factor alone and IC₅₀ values were estimated from two to three separate experiments (*n* = 8–24) using hand drawn probit plots. In each case, the activity of a positive control inhibitor did not deviate more than 10% from the IC₅₀ values listed in the text.

4.7.5. CYQUANT cell proliferation assay

As a measure of cell proliferation, the CYQUANT cell counting/proliferation assay was used as previously described.³⁵ Briefly, cells are first treated with compounds for 12 h and then allowed to grow for an additional 36 h. The cells are then lysed and the CYQUANT dye, which intercalates into the DNA of cells, is added and after 5 min the fluorescence of each well measured using an UV products BioChemi digital darkroom. A positive control used for cytotoxicity in each experiment was cisplatin, with an apparent average IC₅₀ value of 8.2 ± 0.65 μM. Data are graphed as a percent of cells receiving growth factor alone and IC₅₀ values estimated from two to three separate experiments (*n* = 6–15) using probit plots.

4.7.6. CAM assay of angiogenesis

The chorioallantoic membrane (CAM) assay is a standard assay for testing antiangiogenic agents.³⁶ The CAM assay used in these studies was modified from a procedure by Sheu⁴² and Brooks⁴³ and as published previously.⁴⁴ Briefly, fertile leghorn chicken eggs (CBT Farms, Chestertown, MD) are allowed to grow until 10 days of incubation. The proangiogenic factors, human VEGF-165 and bFGF (100 ng each) are then added saturation to a 3 mm microbial testing disk (BBL, Cockeysville, MD) and placed onto the CAM by breaking a small hole in the superior surface of the egg. Antiangiogenic compounds are added 8 h after the VEGF/bFGF at saturation to the same microbial testing disk and embryos allowed to incubate for an additional 40 h. After 48 h, the CAMs are perfused with 2% paraformaldehyde/3% glutaraldehyde containing 0.025% Triton X-100 for 20 s, excised around the area of treatment, fixed again in 2% paraformaldehyde/3% glutaraldehyde for 30 min, placed on petri dishes, and a digitized image taken using a dissecting microscope (Wild M400; Bannockburn, IL) at 7.5X and Retiga enhanced digital imaging system (QImaging, Burnaby, BC, Canada). A grid is then added to the digital CAM images and the average number of vessels within 5–7 grids counted as a measure of vascularity. Semaxanib (**27**) was used as a positive control for antiangiogenic activity. Data are graphed as a percent of CAMs receiving bFGF/VEGF and IC₅₀ values estimated from two to three separate experiments ($n = 5–11$) using nonlinear regression analysis and a Sigmoidal Dose–response analysis using Prism 4.0 (GraphPad Software, San Diego, CA).

4.7.7. Whole animal toxicity assay

To first determine the maximal tolerated dose (MTD) for a twice weekly dose of **8**, male NCr nu/nu mice (4 animals per group) at 8 weeks of age without tumors were injected with 5, 10, 12.5, 15, 17.5 and 20 mg/kg **8** two times weekly, on Monday AM and Thursday PM. Weights were taken and animals observed for acute distress during the first 24 h after injection and animals observed and weighed throughout the 6 week study. It was found that **8** at 20, 17, and 15 mg/kg twice weekly resulted in a significant ($P < 0.05$) weight loss at the 6 week time point. At 12.5 mg/kg twice weekly, a small (1%) but statistically insignificant weight loss occurred and the doses of either 7.5 or 10 mg/kg twice weekly showed no weight loss as compared to their untreated counterparts. The dose of 12.5 mg/kg twice weekly was chosen for the study.

4.7.8. B16-F10 syngeneic tumor model

For this study, 50,000 B16-F10 (lung colonizing) mouse melanoma cells were injected orthotopically SQ just behind the ear of athymic NCr nu/nu male mice, 8 weeks in age. Two experiments were carried out, both starting with five animals per group. Animals were monitored every other day for the presence of tumors. At the time in which most tumors were measurable by calipers (day 8 for this experiment), animals with tumors were randomly sorted into treatment groups and treatment with drugs was initiated. DMSO stock (30 mM) of **8** was further dissolved into sterile water for injection and 12.5 mg/kg injected intraperitoneally (IP) every Monday (AM) and Thursday (PM). Sham treated animals received water only Monday and Thursday. The antifolate methotrexate (MTX) was given at 10 mg/kg every Monday (AM) and Thursday (PM). The length (long side), width (short side) and depth of the tumors were measured using digital Vernier Calipers each Monday, Wednesday, and Friday. Tumor volume was calculated using the formula length \times width \times depth. Tumor growth rate was calculated using a linear regression analysis algorithm using the software GraphPad Prism 4.0.c. At the experiment's end, animals were humanly euthanized using carbon dioxide, tumors and lungs excised, fixed in 20% neutral buffered formalin for 8–10 h,

embedded into paraffin, and hematoxylin–eosin (H&E) stain of three separate tissue sections completed to span the tumor/lung. Metastases per lung lobe counted using the H&E stained sections. The metastases can be seen as purple clusters of disorganized cells on the highly organized largely pink lung. Together with the OUHSC Department of Pathology core, blood vessels per unit area were counted in 5 fields at 100 \times magnification and averaged. Tumor growth rates were compared statistically using two-way ANOVA with a Repeated Measures post-test and tumor vascularity and metastases were compared using one-way ANOVA and a Newman–Keuls post test with the null hypothesis rejected when $P < 0.05$.

4.7.9. Statistics

All analysis was done using Prism 4.0. (GraphPad Software, San Diego, CA.)

Acknowledgments

This work was supported, in part, by the National Institutes of Health, National Cancer Institute Grant CA98850 (A.G.) and the Duquesne University Adrian Van Kaam Chair in Scholarly Excellence (AG).

Supplementary data

Supplementary data associated with this article can be found, in the online version, at <http://dx.doi.org/10.1016/j.bmc.2012.12.045>.

References and notes

- Herbst, R. S.; Fukuoka, M.; Baselga, J. *Nat. Rev. Cancer* **2004**, *4*, 956.
- Ellis, L. M. *Hematol. Oncol. Clin. North Am.* **2004**, *18*, 1007.
- Jain, R. K. *Semin. Oncol.* **2002**, *29*, 3.
- Ferrara, N. *Semin. Oncol.* **2002**, *29*, 10.
- Taberero, J. *Mol. Cancer Res.* **2007**, *5*, 203.
- Folkman, J. *Annu. Rev. Med.* **2006**, *57*, 1.
- Vacca, A.; Ribatti, D. *Leukemia* **2006**, *20*, 193.
- Schuch, G.; Oliveira-Ferrer, L.; Loges, S.; Laack, E.; Bokemeyer, C.; Hossfeld, D. K.; Fiedler, W.; Ergun, S. *Leukemia* **2005**, *19*, 1312.
- Koster, A.; Raemaekers, J. M. *Curr. Opin. Oncol.* **2005**, *17*, 611.
- Quesada, A. R.; Munoz-Chapuli, R.; Medina, M. A. *Med. Res. Rev.* **2006**, *26*, 483.
- Comis, R. L. *Oncologist* **2005**, *10*, 467.
- Faivre, S.; Djelloul, S.; Raymond, E. *Semin. Oncol.* **2006**, *33*, 407.
- Bergers, G.; Song, S.; Meyer-Morse, N.; Bergsland, E.; Hanahan, D. *J. Clin. Invest.* **2003**, *111*, 1287.
- Erber, R.; Thurnher, A.; Katsen, A. D.; Groth, G.; Kerger, H.; Hammes, H. P.; Menger, M. D.; Ullrich, A.; Vajkoczy, P. *FASEB J.* **2004**, *18*, 338.
- Shen, J.; Vil, M. D.; Zhang, H.; Tonra, J. R.; Rong, L. L.; Damoci, C.; Prewett, M.; Deevi, D. S.; Kearney, J.; Surguladze, D.; Jimenez, X.; Iacolina, M.; Bassi, R.; Zhou, K.; Balderes, P.; Mangalampalli, V. R.; Loizos, N.; Ludwig, D. L.; Zhu, Z. *Biochem. Biophys. Res. Commun.* **2007**, *357*, 1142.
- Gille, H.; Kowalski, J.; Li, B.; LeCouter, J.; Moffat, B.; Zioncheck, T. F.; Pelletier, N.; Ferrara, N. *J. Biol. Chem.* **2001**, *276*, 3222.
- Marcucci, G.; Perrotti, D.; Caligiuri, M. A. *Clin. Cancer Res.* **2003**, *9*, 1248.
- Chow, L. Q.; Eckhardt, S. G. *J. Clin. Oncol.* **2007**, *25*, 884.
- Gridelli, C.; Maione, P.; Del Gaizo, F.; Colantuoni, G.; Guerriero, C.; Ferrara, C.; Nicoletta, D.; Comunale, D.; De Vita, A.; Rossi, A. *Oncologist* **2007**, *12*, 191.
- Nelson, M. H.; Dolder, C. R. *Ann. Pharmacother.* **2006**, *40*, 261.
- Gangjee, A.; Yang, J.; Ihnat, M. A.; Kamat, S. *Bioorg. Med. Chem.* **2003**, *11*, 5155.
- Gangjee, A.; Namjoshi, O. A.; Yu, J.; Ihnat, M. A.; Thorpe, J. E.; Warnke, L. A. *Bioorg. Med. Chem.* **2008**, *16*, 5514.
- Gangjee, A.; Namjoshi, O. A.; Ihnat, M. A.; Buchanan, A. *Bioorg. Med. Chem. Lett.* **2010**, *20*, 3177.
- Mazitschek, R.; Giannis, A. *Curr. Opin. Chem. Biol.* **2004**, *8*, 432.
- Isanbor, C. O. H. D. *J. Fluor. Chem.* **2006**, *127*, 303.
- Rewcastle, G. W.; Denny, W. A.; Bridges, A. J.; Zhou, H.; Cody, D. R.; McMichael, A.; Fry, D. W. *J. Med. Chem.* **1995**, *38*, 3482.
- Bridges, A. J.; Zhou, H.; Cody, D. R.; Rewcastle, G. W.; McMichael, A.; Showalter, H. D.; Fry, D. W.; Kraker, A. J.; Denny, W. A. *J. Med. Chem.* **1996**, *39*, 267.
- Wissner, A.; Berger, D. M.; Boschelli, D. H.; Floyd, M. B., Jr.; Greenberger, L. M.; Gruber, B. C.; Johnson, B. D.; Mamuya, N.; Nilakantan, R.; Reich, M. F.; Shen, R.; Tsou, H. R.; Upeslaciis, E.; Wang, Y. F.; Wu, B.; Ye, F.; Zhang, N. *J. Med. Chem.* **2000**, *43*, 3244.
- Yun, C. H.; Boggon, T. J.; Li, Y.; Woo, M. S.; Greulich, H.; Meyerson, M.; Eck, M. J. *Cancer Cell* **2007**, *11*, 217.

30. Manley, P. W.; Furet, P.; Bold, G.; Bruggen, J.; Mestan, J.; Meyer, T.; Schnell, C. R.; Wood, J.; Haberey, M.; Huth, A.; Kruger, M.; Menrad, A.; Ottow, E.; Seidelmann, D.; Siemeister, G.; Thierauch, K. H. *J. Med. Chem.* **2002**, *45*, 5687.
31. Gangjee, A.; Yu, J.; Kisliuk, R. L. *J. Heterocycl. Chem.* **2002**, *39*, 833.
32. Fong, T. A.; Shawver, L. K.; Sun, L.; Tang, C.; App, H.; Powell, T. J.; Kim, Y. H.; Schreck, R.; Wang, X.; Risau, W.; Ullrich, A.; Hirth, K. P.; McMahon, G. *Cancer Res.* **1999**, *59*, 99.
33. Stockwell, B. R.; Haggarty, S. J.; Schreiber, S. L. *Chem. Biol.* **1999**, *6*, 71.
34. Schilder, R. J.; Hall, L.; Monks, A.; Handel, L. M.; Fornace, A. J., Jr.; Ozols, R. F.; Fojo, A. T.; Hamilton, T. C. *Int. J. Cancer* **1990**, *45*, 416.
35. Wilson, S. M.; Barsoum, M. J.; Wilson, B. W.; Pappone, P. A. *Cell Prolif.* **1999**, *32*, 131.
36. Vu, M. T.; Smith, C. F.; Burger, P. C.; Klintworth, G. K. *Lab. Invest.* **1985**, *53*, 499.
37. Soucy, N. V.; Ihnat, M. A.; Kamat, C. D.; Hess, L.; Post, M. J.; Klei, L. R.; Clark, C.; Barchowsky, A. *Toxicol. Sci.* **2003**, *76*, 271.
38. Fidler, I. J. *Cancer Res.* **1975**, *35*, 218.
39. Fidler, I. J.; Gersten, D. M.; Budmen, M. B. *Cancer Res.* **1976**, *36*, 3160.
40. Fidler, I. J.; Nicolson, G. L. *Isr. J. Med. Sci.* **1978**, *14*, 38.
41. Poste, G.; Doll, J.; Hart, I. R.; Fidler, I. J. *Cancer Res.* **1980**, *40*, 1636.
42. Sheu, J. R.; Fu, C. C.; Tsai, M. L.; Chung, W. J. *Anticancer Res.* **1998**, *18*, 4435.
43. Brooks, P. C.; Montgomery, A. M.; Cheresch, D. A. *Methods Mol. Biol.* **1999**, *129*, 257.
44. Marks, M. G.; Shi, J.; Fry, M. O.; Xiao, Z.; Trzyna, M.; Pokala, V.; Ihnat, M. A.; Li, P. K. *Biol. Pharm. Bull.* **2002**, *25*, 597.